DOI: 10.61782/fa.2025.0496

INVESTIGATING SPATIAL ALIASING AND FRESNEL ZONES OF LINE AND PLANAR SOURCES FOR SOUND REINFORCEMENT

Lukas Gölles[1,2*] **Franz Zotter**[1,2]
[1] Institute of Electronic Music and Acoustics, Graz, Austria
[2] University of Music and Performing Arts, Graz, Austria

ABSTRACT

Modern large-scale sound reinforcement systems predominantly utilize line-source arrays and, more recently, planar matrix arrays due to their flexibility in shaping direct sound pressure coverage across the listening area. In these arrays, the received sound pressure level is influenced, not only by the listener's distance, but also by the size of the first Fresnel Zone on the array, particularly around the origin of the earliest wavefront. The size of this zone varies with both frequency and source dimensions, and it can be adjusted through curvature and time delays. However, comb filtering effects inevitably arise, especially at higher frequencies, due to contributions from later Fresnel Zones and the finite size of the array. Additionally, the discrete spacing of drivers in both line and planar sources introduces spatial aliasing. This contribution presents simulations that analyze the impact of Fresnel Zones, driver spacing, and driver arrangements on frequency response and direct sound coverage within the listening area.

Keywords: *line array, planar arrays, spatial aliasing, Fresnel Zones, sound reinforcement*

1. INTRODUCTION

The field of sound reinforcement is fundamentally concerned with the precise reproduction, control, and propagation of sound waves to ensure optimal audio quality and spatial fidelity. Line-source arrays have long been the standard for large-scale sound reinforcement systems, but more recently, planar arrays have also gained prominence. In this context, spatial aliasing and Fresnel Zones play an essential role in shaping the performance of sound systems. These phenomena are central to the design and operation of modern sound reinforcement systems and present significant challenges that must be addressed to guarantee high-fidelity audio reproduction across diverse environments, ranging from concert halls to outdoor venues.

Fresnel Zones, derived from wave interference theory, define regions of constructive and destructive interference that arise as sound waves propagate from a linear or planar source to a receiver. These zones are particularly relevant in large-scale sound reinforcement, where the interaction of wavefronts over extended distances can result in variations in sound pressure levels and phase coherence. The concept of Fresnel Zones, initially developed in optical theory to describe the diffraction of light waves [1], has proven to be an invaluable tool in acoustics for understanding how sound waves interact with physical obstacles and how these interactions influence perceived sound quality. Notably, Kuttruff's work [2] underscores the importance of Fresnel Zones in room acoustics, emphasizing their role in shaping the spatial distribution of sound energy and the clarity of audio signals. In sound reinforcement systems, effective consideration of Fresnel Zones is critical for minimizing interference effects and ensuring uniform coverage, especially in line and planar array configurations.

Spatial aliasing, in contrast, occurs when the spatial sampling of sound sources is inadequate to excite the wave field with sufficient continuity. This issue is particularly prominent in line and planar sound sources, where the discrete arrangement of transducers can introduce artifacts and distortions in the reproduced sound. Berkhout et al. [3] provide a foundational understanding of spatial aliasing in array-based sound systems, demonstrating how

**Corresponding author*: *goelles@iem.at.*

transducer spacing and the frequency content of sound signals contribute to aliasing phenomena. Line arrays, composed of multiple closely spaced transducers arranged in a vertical configuration, are widely used in sound reinforcement for their ability to provide controlled directivity and extended range. However, the discrete nature of line arrays makes them vulnerable to spatial aliasing, particularly at higher frequencies. Heil et al. and Urban et al. offer valuable insights into the properties of arrays composed by multiple sources and outline five essential criteria that line arrays must satisfy [4, 5]. Planar arrays, which extend line arrays into two dimensions, encounter similar challenges, albeit with greater complexity due to the increased number of transducers and the multidimensional nature of wave propagation.

This paper explores the effects of Fresnel Zones and spatial aliasing in the context of linear and planar sound sources, focusing on their implications for sound reinforcement systems. The goal is to offer a comprehensive understanding of the challenges they present and the strategies available to mitigate their impact on the listening area. Through a combination of theoretical analysis and numerical simulations, we will demonstrate how optimizing transducer spacing, array geometry, and signal processing algorithms can enhance sound quality and spatial fidelity in practical applications.

2. PHASED LINE SOURCE

2.1 Line Source Phasing

Recently, a theory for line array curving and phasing has been introduced [6], presenting a nonlinear differential equation for the total inclination $\vartheta_\mathrm{T} = a\,\vartheta + (1-a)\,\vartheta_\mathrm{w}$ which is linearly decomposed into a curving component ϑ and a phasing/beamforming component ϑ_w,

$$\dot{\vartheta}_\mathrm{T} = -\frac{r^{2\,\beta}}{g^2}\frac{1}{r^2\,\cos\vartheta_\mathrm{w}} + \frac{\cos\vartheta_\mathrm{w}}{r}\,, \qquad \text{with } r = \frac{z}{\sin\vartheta_\mathrm{T}}\,. \tag{1}$$

Here, r represents the distance between the source and receiver, and z is the current z-coordinate of the source when solving the differential equation stepwise. The parameter g determines the radius of curvature at the highest point, while β is a design parameter controlling the direct sound level roll-off, resulting in a decay of $-6\cdot\beta$ dB per distance doubling (dod) across the listening area. Using the Frenet-Serret formulas, which describe arbitrary spatial trajectories, the tangent at any point on the curved line source is given by $\boldsymbol{t} = \begin{bmatrix}\sin\vartheta & 0 & \cos\vartheta\end{bmatrix}^\mathsf{T}$. The geometry of the source is then computed by integrating along the natural source length parameter,

$$\boldsymbol{x}(s) = \int_0^S \boldsymbol{t}\,\mathrm{d}s + \boldsymbol{x}_0 \qquad \boldsymbol{x}_0 = \begin{bmatrix}0 & 0 & z_0\end{bmatrix}^\mathsf{T}\,, \tag{2}$$

where z_0 defines the mounting height of the line source. The delay introduced along the curve acts as a progressive delay and summing beamformer, with the delay length determined by integrating over the sine,

$$w = -\int_0^S \sin\vartheta_\mathrm{w}\,\mathrm{d}s\,. \tag{3}$$

It has been shown, that this formalism is directly applicable to line-array curvature design after discretization [7]. Furthermore, for optimal frequency homogeneity across distance and a balanced trade-off between preserving the mixing balance and enhancing envelopment in immersive sound reinforcement at off-center listening positions, it is recommended to use line sources with a direct sound level decay of -1.5 dB/dod [8]. Accordingly, the simulations in this study are conducted for sources exhibiting this specific decay characteristic.

2.2 Simulation Procedure

We consider a mid-scale sound reinforcement scenario. To align with the results presented in [6], we employ a linear arrangement of the line array prototype [9] consisting of 12 elements.

The continuous line source contour, along with the phasing profile,cf. Eq. (1), (2), and (3), is computed through numerical simulation, following Algorithm 1 in [6]. The simulation parameters are set as follows: $x_{r,0} = 10\,\mathrm{m}$, $z_0 = 2\,\mathrm{m}$, $g = 0.4093$, and $\beta = 0.25$. The phasing profile is discretized based on the element height of the line array prototype, which measures $8.2\,\mathrm{cm}$ [9].

To simulate a piston-shaped driver, we employ a circular arrangement of ideal point sources positioned at $1\,\mathrm{mm}$ intervals. Each source is described using Green's function, with a total diameter of $6.35\,\mathrm{cm}$ (2.5 inches). A Gaussian filter is applied as an amplitude kernel to each element, under the assumption that the driver's edge contributes less to radiation than its center,

$$K[m,n] = \left[e^{-\frac{m^2+n^2}{2\,\sigma^2}}\right]^5\,. \tag{4}$$

Here, σ^2 represents the standard deviation, defining the width of the Gaussian kernel, and is set to $\sigma = 0.83$.

The exponent of five is chosen based on simulation results from [6,10], as there the results of the measurement match well to the simulation using the prototype array of [9].
For equalization, a filter is applied whose magnitude increases by 3 dB per octave up to the spatial aliasing frequency, compensating for the pink frequency response characteristic of a line source composed of ideal point sources, as described in [6].
At each observation point, the sound pressure is evaluated over a frequency range from 20 Hz to 24 kHz with a linear resolution of 512 points. To visualize the coverage as a broadband result, the frequency responses are third-octave smoothed, followed by A-weighting before summation.

2.3 Spatial Aliasing

Fig. 1 presents the simulated frequency responses of discrete line sources composed of 12 elements. Due to the driver spacing of 8.2 cm, spatial aliasing is expected to occur at approximately $f_{\mathrm{spat.al}} \approx 4.2\,\mathrm{kHz}$ which is clearly reflected in the graphs.
The impact of spatial aliasing can potentially be mitigated through the use of waveguides, f.e. DOSC (Diffuseur d'onde sonor cylindrique [11]), HRW (Hyperbolic Reflective Waveguide [12]), or multi-driver systems. A key advantage of a multiway system incorporating smaller drivers for high frequencies is, that the required curvature of the outlet for near-field sound reinforcement can be more effectively achieved due to the closer spacing of the drivers.
Fig. 2 illustrates the simulated on-axis frequency responses at various distances for a two-way system. In this setup, 2.5-inch drivers spaced at 8.2 cm intervals are used for the lower frequencies, while 1-inch drivers positioned at 2.9 cm intervals handle the higher frequencies. The crossover frequency is set at 2 kHz, and each filter (high-pass and low-pass) is a 4th-order Butterworth filter with a cutoff frequency at 2 kHz. Notably, the two-way system increases the spatial aliasing frequency to approximately 14 kHz due to the reduced driver spacing.

2.4 Fresnel Zones

Figures 3 and 4 illustrate the sizes of the various Fresnel Zones for a discrete line source with 12 elements at the observation points $\boldsymbol{x}_{\mathrm{r}} = \begin{bmatrix}1 & 0 & 0\end{bmatrix}^{\mathsf{T}}$ and $\boldsymbol{x}_{\mathrm{r}} = \begin{bmatrix}2 & 0 & 0\end{bmatrix}^{\mathsf{T}}$. The regions marked in black represent the first Fresnel Zone, which is the most significant. As the zone number increases, the regions become progressively brighter. For clarity, only the first five Fresnel Zones are depicted.

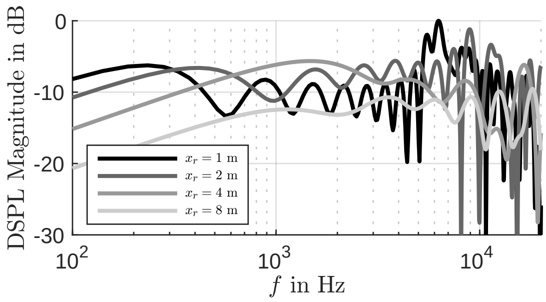

Figure 1. On-axis frequency responses of a 12-element discrete line array at different distances to the source.

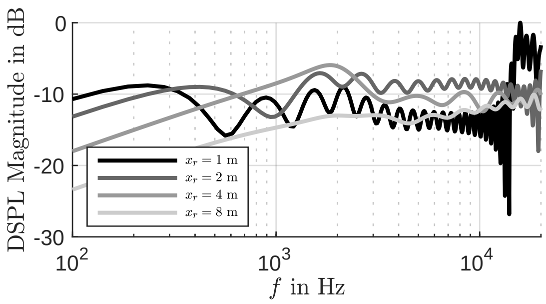

Figure 2. On-axis frequency responses of a 12-element discrete line array (two way system) at different distances to the source.

At both observation points, the Fresnel Zones exhibit asymmetry. At $x_{\mathrm{r}} = 1\,\mathrm{m}$, the second Fresnel Zone becomes evident at 500 Hz, contributing to the first notch in the frequency response, as shown in Fig. 1. As the frequency increases, the Fresnel Zone diminishes in size, resulting in comb filtering effects in the frequency response. At $x_{\mathrm{r}} = 2\,\mathrm{m}$, the entire source lies within the first Fresnel Zone. The size of the first Fresnel Zone at 1 kHz at $x_{\mathrm{r}} = 2\,\mathrm{m}$ is comparable to that at 500 Hz for $x_{\mathrm{r}} = 1\,\mathrm{m}$. This causes a shift in the first notch to approximately 1 kHz, resulting in an additional comb filter pattern.
Tapering, a well known technique from phased antenna theory [13] and also known as shading in the theory of constant-beamwidth transducer in acoustics [14], can be applied to the array to mitigate the effects of comb filtering. Fig. 5 presents the on-axis frequency responses at different distances of the dual-driver array, consisting of 12 low-frequency drivers and 33 high-frequency drivers, with amplitude tapering applied. For amplitude tapering,

we used a Hann window

$$a[n] = \frac{1}{2}\left(1 - \cos\frac{2\,\pi\,n}{M-1}\right)\,, \tag{5}$$

where the window length M is chosen such that the outermost element is attenuated by $10\,\mathrm{dB}$. This condition is expressed as $a\left[\frac{(M+1)}{2} - \frac{N}{2}\right] = 10^{\frac{-10}{20}}$, where N denotes the number of array elements. By rearranging Eq. (5), the required parameter M is determined

$$M = \mathrm{rd}\left\{\frac{\pi\,(N+1) - \arccos\left(1 - 2\cdot 10^{\frac{-10}{20}}\right)}{\pi - \arccos\left(1 - 2\cdot 10^{\frac{-10}{20}}\right)}\right\}. \tag{6}$$

Subsequently, only the symmetric section centered around the peak of the window function is utilized, ensuring it aligns with the number of array elements N. While this tapering results in a noticeable reduction of the notches in the frequency response, it also limits the coverage area, leading to excessively small levels at close observation points, as seen in Fig. 7.
To increase coverage (with $g = 0.38$) while maintaining tapering such that the closest desired observation point is closer to the source, i.e., $x_r = -0.14\,\mathrm{m}$, frequency responses similar to those in Fig. 5 are achieved, c.f. Fig. 6. Additionally, the A-weighted sum of the direct sound level over the distance is comparable to the setup without tapering, as shown in Fig. 7.

3. PHASED PLANAR SOURCES

3.1 Planar Source Phasing

The formalism introduced in [6] has been extended to planar arrays in [10] by introducing a horizontal spread parameter a and a lateral distance range parameter b as design parameters in addition to g and β. Since implementing a two-dimensional curved source is challenging, the proposed method relies on flat planar sources, where delays are used to achieve the desired $-6\cdot\beta$ dB/dod in the listening area. The formalism employs a set of three differential equations to calculate the delay length $w = c\cdot\tau$, where c represents the speed of sound and τ denotes the

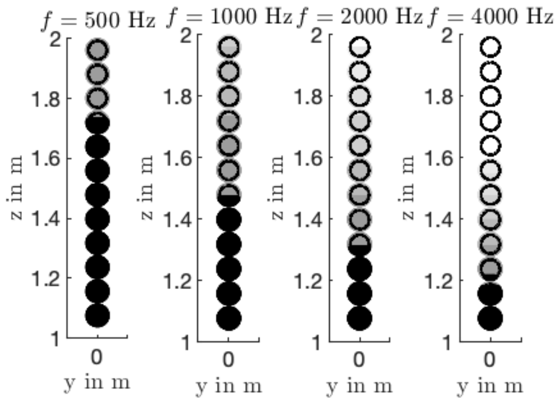

Figure 3. Fresnel Zones (1st=black) on the source at observation point at $x_\mathrm{r} = 1\,\mathrm{m}$ for different frequencies.

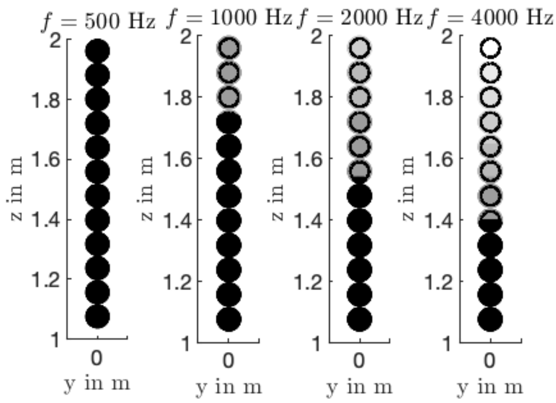

Figure 4. Fresnel Zones on the source at observation point at $x_\mathrm{r} = 2\,\mathrm{m}$ for different frequencies.

equivalent delay:

$$\frac{\partial^2 w}{\partial h^2} = a + \frac{1}{r}\left(\frac{\partial w}{\partial h}\right)^2 \tag{7}$$

$$\frac{\partial^2 w}{\partial h\,\partial v} = b + \frac{1}{r}\frac{\partial w}{\partial h}\,\frac{\partial w}{\partial v} \tag{8}$$

$$\frac{\partial^2 w}{\partial v^2} = \frac{1}{r}\left[\frac{g^{-2}\,r^{2\beta} + r^2\,b^2}{1 + r\,a} + \left(\frac{\partial w}{\partial v}\right)^2 - 1\right] \tag{9}$$

with $r = \dfrac{v\,\cos\eta + z_0}{-\frac{\partial w}{\partial v}\,\cos\eta + \sin\eta\,\sqrt{1 - \left(\frac{\partial w}{\partial h}\right)^2 - \left(\frac{\partial w}{\partial v}\right)^2}}$.

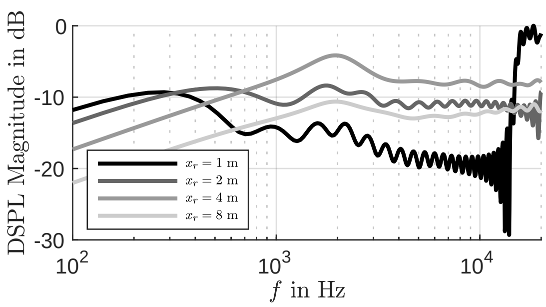

Figure 5. On-axis frequency responses of a 12-element discrete line array (two way system) at different distances to the source with applied tapering.

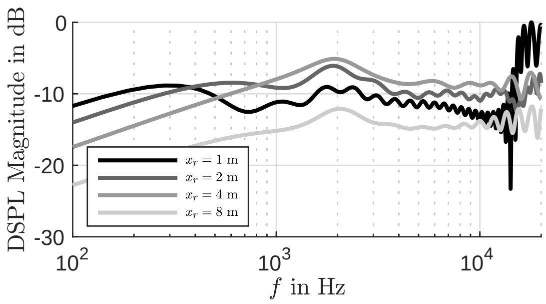

Figure 6. On-axis frequency responses of a 12-element discrete line array (two way system) at different distances to the source with applied tapering and modified coverage.

Here, η denotes the inclination of the planar source, v defines the source length in the vertical direction (i.e., $v \in [0, -V]$), and h represents the width in the horizontal direction ($h \in \left[-\frac{H}{2}, \frac{H}{2}\right]$). z_0 is the mounting height of the planar source, which corresponds to the distance between the highest point of the source and the listening area (assumed to be on the x-y plane). The geometry of the planar source is described using the unit vectors $\boldsymbol{e}_\mathrm{h} = \begin{bmatrix} 0 & 1 & 0 \end{bmatrix}^\mathsf{T}$ and $\boldsymbol{e}_\mathrm{v} = \begin{bmatrix} \sin\eta & 0 & \cos\eta \end{bmatrix}^\mathsf{T}$,

$$\boldsymbol{x}_\mathrm{s} = \boldsymbol{x}_0 + h\,\boldsymbol{e}_\mathrm{h} + v\,\boldsymbol{e}_\mathrm{v} \qquad \text{with } \boldsymbol{x}_0 = \begin{bmatrix} 0 & 0 & z_0 \end{bmatrix}^\mathsf{T}. \tag{10}$$

3.2 Simulation Procedure

To make the results from both sources comparable, a planar source with 9×10 elements of size $8.2\,\mathrm{cm} \times 8.2\,\mathrm{cm}$

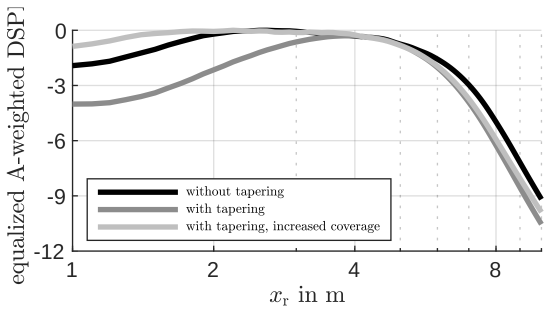

Figure 7. Equalized A-weighted direct sound level in ox-axis direction.

is chosen. The differential equations (7), (8), and (9) are solved numerically, following Algorithm 3 from [10], using the parameters $x_{\mathrm{z},0} = 10\,\mathrm{m}$, $z_0 = 2\,\mathrm{m}$, $\eta = 11.3°$, $\beta = 0.25$, $g = 0.2492$, $a = 1.9684$, and $b = 0.3902$. The parameters a and b control the coverage width, while η defines the total inclination of the source. In this case, an outermost observation point at $\boldsymbol{x}_\mathrm{r} = \begin{bmatrix} 5 & 5 & 0 \end{bmatrix}^\mathsf{T}$ is targeted. The values of a and b are derived from a fixed-point iteration as described in Algorithm 1 of [10]. Subsequently, the phasing profile is discretized as proposed in [10].
The individual elements are simulated in the same manner as the linear sources described earlier.

3.3 Spatial Aliasing

Spatial aliasing presents challenges similar to those encountered with linear sources. The top panel of Fig. 8 displays the frequency responses at various observation points. However, for practical reasons, employing an array with smaller, more densely spaced drivers is not a viable solution, as smaller drivers are generally less effective at reproducing lower frequencies. Additionally, a two-way system with an auxiliary array of smaller, denser drivers positioned in front of the main array is not feasible, as it would adversely affect the radiation of lower frequencies. A possible approach to mitigate spatial aliasing effects, at least along the depth dimension, involves placing a vertical array of smaller, densely packed drivers in front of each vertical loudspeaker line. Fig. 8 compares the frequency responses of an array using $2.5\,\mathrm{inch}$ drivers across the entire frequency range to an alternative array that employs $2.5\,\mathrm{inch}$ drivers for lower frequencies and $1\,\mathrm{inch}$ drivers for higher frequencies. The crossover frequency is set at $2\,\mathrm{kHz}$, with each filter (high-pass and low-

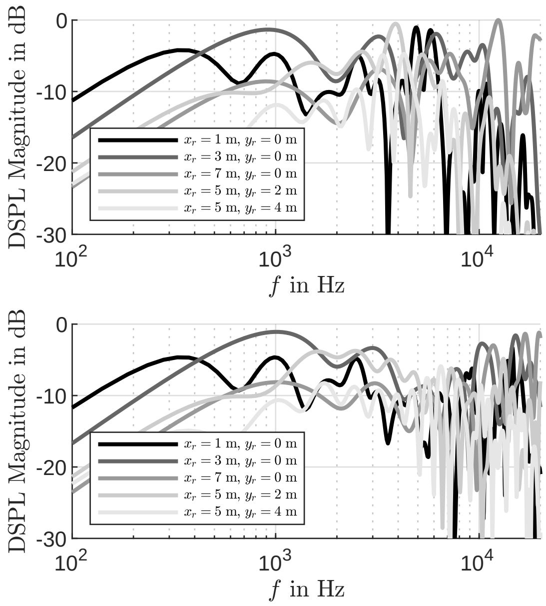

Figure 8. Comparing the frequency responses of a planar array as one-way system (top) and a two-way system (bottom) at different observation points that lie within the desired coverage region.

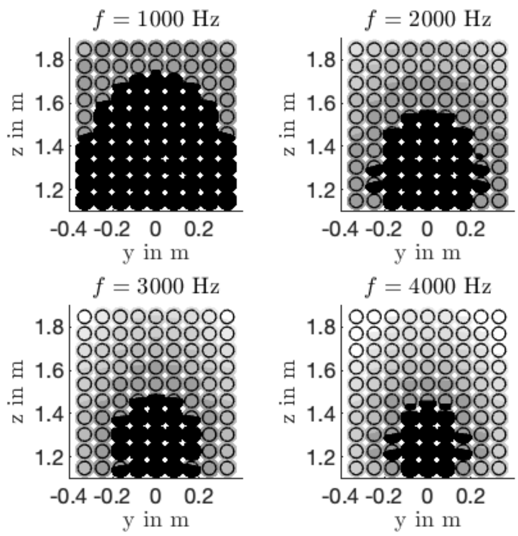

Figure 9. Fresnel Zones on the source at observation point at $\boldsymbol{x}_{\mathrm{r}} = \begin{bmatrix} 2 & 0 & 0 \end{bmatrix}^{\mathsf{T}}$ for different frequencies.

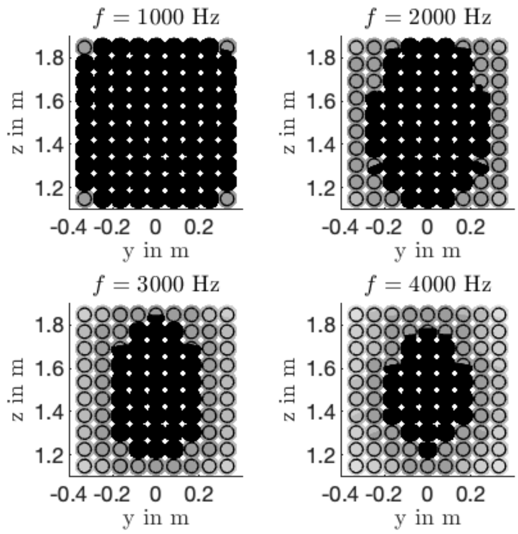

Figure 10. Fresnel Zones on the source at observation point at $\boldsymbol{x}_{\mathrm{r}} = \begin{bmatrix} 4 & 0 & 0 \end{bmatrix}^{\mathsf{T}}$ for different frequencies.

pass) implemented as a 4th-order Butterworth filter with a cutoff frequency of 2 kHz. Notable improvements in the frequency response are observed in the range of 3 kHz to 6 kHz. However, spatial aliasing at high frequencies remains unavoidable.

3.4 Fresnel Zones

Figures 9 and 10 depict the Fresnel Zones on the planar source at various frequencies for two different observation points. As with the line sources, it is observed that nearly the entire source lies within the first Fresnel Zone at 1 kHz for both observation points. For other frequencies, the size and shape of the Fresnel Zones vary with distance. The observed discontinuities in the zones arise from the fact that the phase profile of an element has been discretized, and the Fresnel Zone is calculated for multiple points on the driver. Consequently, only part of the driver falls within one Fresnel Zone, while the remainder belongs to the next higher Fresnel Zone.
As previously conducted for line sources, tapering is applied to mitigate the effects of comb filtering. The top panel of Fig. 11 illustrates the frequency responses at various observation points for the phased planar source without tapering. The center panel presents the corresponding results after tapering is applied. The same window function as for line sources was selected for tapering, but the outermost elements were attenuated only by 6 dB in both

the horizontal and vertical directions.
Similar to line sources, the implementation of tapering enhances the frequency response below the aliasing frequency but simultaneously reduces the coverage area, comparing the top and center panels of Fig. 12. To address this limitation, the coverage can be strategically designed for a broader region by adjusting the parameters defining the horizontal coverage to $a = 2.295$ and $b = 0.2919$, thereby targeting an outermost observation point at $\boldsymbol{x}_{\mathrm{r}} = \begin{bmatrix} 5 & 8 & 0 \end{bmatrix}^{\mathsf{T}}$. Additionally, the nearest observation point is repositioned to $x_{\mathrm{r}} = 0.22\,\mathrm{m}$. A comparison of the results indicates that the coverage achieved with these modifications is comparable to that of the untapered source, cf. Fig. 12. The frequency response characteristics of the tapered source exhibit noticeable improvements, cf. Fig. 11.

4. CONCLUSION

This contribution investigated the effects of spatial aliasing and Fresnel Zones for both line and planar sources in sound reinforcement systems. To improve the frequency responses, tapering can be applied; however, this comes with the trade-off of restricting the coverage area. It was demonstrated that designing for an extended area yields similar results in terms of the covered region when compared to the source without tapering, but with the added improvements in the frequency response achieved through the application of tapering.
Further research should focus on measuring the prototype array and comparing the simulation results with practical applications. Additionally, the impact of individual filtering of the array enclosure should be explored to determine whether further improvements in coverage and frequency homogeneity over distance can be achieved.

5. ACKNOWLEDGMENTS

Our research was funded by the Austrian Science Fund (FWF): P 35254-N (Envelopment in Immersive Sound Reinforcement, EnImSo).

6. REFERENCES

[1] A. Fresnel, “Mémoire sur la diffraction de la lumière,” in *Annales de Chimie et de Physique*, 1816.

[2] H. Kuttruff, *Room Acoustics, Fourth Edition*. E-Libro, Taylor & Francis, 2000.

[3] A. J. C. Berkhout, D. de Vries, and P. Vogel, “Acoustic control by wave field synthesis,” *Journal of the Acoustical Society of America*, vol. 93, pp. 2764–2778, 1993.

[4] C. Heil and M. Urban, “Sound fields radiated by multiple sound sources arrays,” in *Audio Engineering Society Convention 92*, Mar 1992.

[5] M. Urban, C. Heil, and P. Bauman, “Wavefront sculpture technology,” *J. Audio Eng. Soc*, vol. 51, no. 10, pp. 912–932, 2003.

[6] L. Gölles and F. Zotter, “Theory of continuously curved and phased line sources for sound reinforcement,” *Acta Acust.*, vol. 7, p. 52, 2023.

[7] L. Gölles and F. Zotter, “Dual-target design for large-scale sound reinforcement: Simulation and evaluation,” in *Audio Engineering Society Conference: AES 2024 International Conference on Acoustics & Sound Reinforcement*, Jan 2024.

[8] L. Gölles, M. Frank, and F. Zotter, “Evaluating a dual-target line-array design for medium-scale surround sound reinforcement,” in *Audio Engineering Society Convention 156*, (Madrid), 06 2024.

[9] L. Gölles, F. Zotter, and L. Merkel, “Miniature line array for immersive sound reinforcement,” in *Proceedings of AES SIA Conf.*, (Huddersfield), 08 2023.

[10] L. Gölles and F. Zotter, “Theory of continuously phased planar sources for sound reinforcement,” *Acta Acust.*, vol. 8, p. 77, 2024.

[11] C. Heil, “Sound wave guide,” U.S. Patent 5163167A, Oct. 1992.

[12] E. Vincenot and F. Deffarges, “Sound-Producing Device With Acoustic Waveguide,” U.S. Patent 6585077B2, Jul. 2003.

[13] R. Mailloux, *Phased Array Antenna Handbook*. Antennas and Propagation Library, Artech House, 2005.

[14] taylor richard, manke kurtis, and keele d.b. (don), “circular-arc line arrays with amplitude shading for constant directivity,” *journal of the audio engineering society*, vol. 67, pp. 400–413, june 2019.

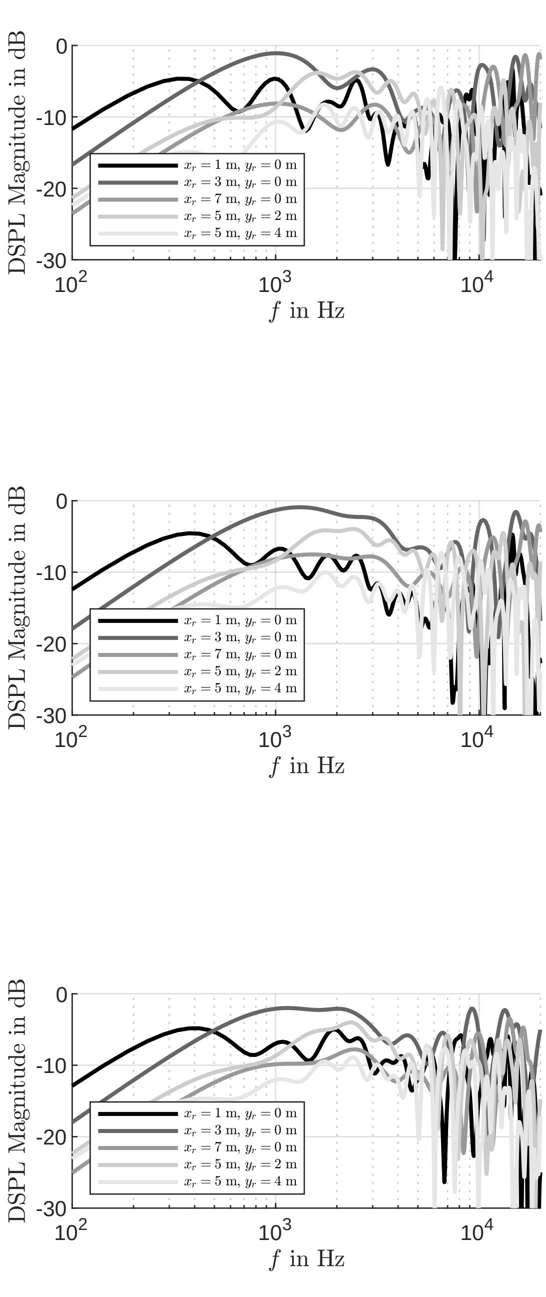

Figure 11. Frequency responses of a planar array at different observation points that lie within the desired coverage region.

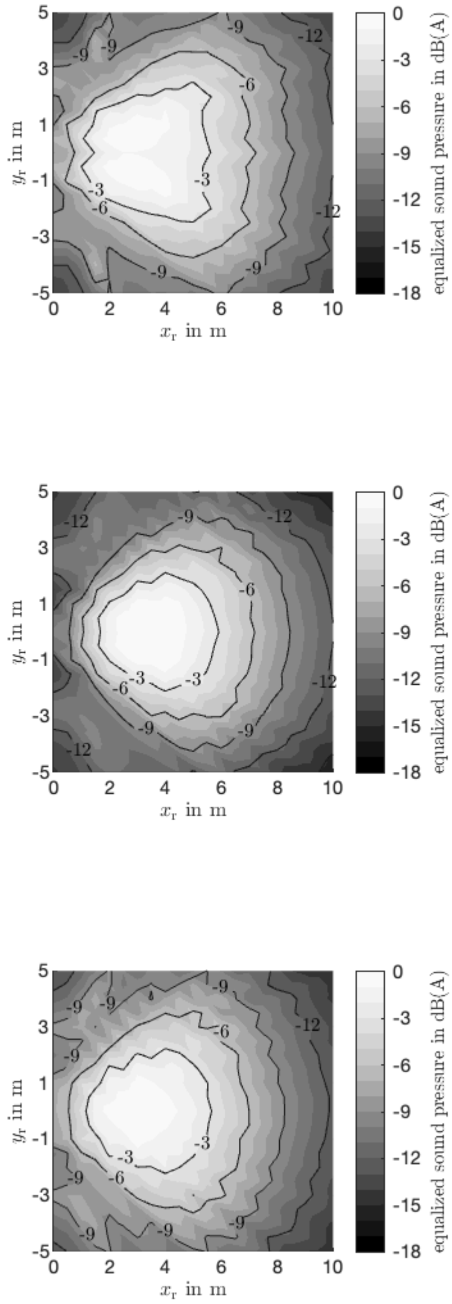

Figure 12. Equalized A-weighted direct sound level in ox-axis direction with applied tapering.